The 2009 IEEE/RSJ International Conference on
Intelligent Robots and Systems
October 11-15, 2009 St. Louis, USA

Local Scan for Compensation of Drift Contamination in AFM Based Nanomanipulation

Yucai Wang and Guangyong Li
Department of Electrical and Computer Engineering
University of Pittsburgh
Pittsburgh, Pennsylvania 15261, USA
{ yuw19+ & gul6+}@pitt.edu

Lianqing Liu
State Key Laboratory of Robotics
Shenyang Institute of Automation
Shenyang, Liaoning Province 110016, China
lqliu@sia.cn

***Abstract* – Because of the presence of thermal drift, AFM (atomic force microscopy) images are always contaminated. Such contamination is one of the major hampers to achieve accurate and efficient AFM based nanomanipulation. Based on contaminated images, the manipulation operations often fail. In this paper, we apply a local scan method to identify and compensate the thermal drift contamination in the AFM image. After an AFM image is captured, the entire image is divided into several parts along y direction. A local scan is immediately performed in each part of the image to calculate the drift value at that very part. In this manner, the drift value is calculated in a small local area instead of the global image. Thus, the drift can be more precisely estimated and the image can be more accurately recovered, which lead to improved accuracy for AFM imaging and enhanced productivity for AFM based nanomanipulation.**

Index Terms - Nanomanipulation, Atomic Force microscope, Drift Compensation.

I. INTRODUCTION

After more than 20 years' development, AFM (atomic force microscope) [1] has not only been proven a powerful tool in characterizing various samples surface down to the nanometer scale, but also demonstrated the capability of modifying surfaces through nanolithography [2-3] and nanomanipulation [3-4], which is a promising nano-fabrication technique that combines both "top-down" and "bottom-up" advantages [5]. AFM based nanomanipulations have been intensively studied in recent years [6-14] and various kinds of manipulation schemes have been proposed in last decade. Nowadays, manipulation of particles with diameters of ~10nm using AFM is being investigated by many research groups [14-17]. Nanomanipulation operations are routinely used to precisely control atoms, molecules or nanoscale objects to fabricate nanodevices and to repair or modify nanostructures formed by other methods.

There are several hampers to accomplish successful AFM based nanomanipulation. correction [18]. When nanomanipulations are performed in ambient conditions without rigorous environmental controls, thermal drift becomes one of the hurdles to precisely locate targets due to the drift contamination to AFM image. Solving the problem of drift contamination is the primary step towards accurate and efficient automated manipulation. Thermal drift cannot be compensated by the closed-loop feedback equipped in modern AFM system for compensation of hysteresis and creep effects [19]. Many researchers have tried to address drift contamination issue [20-24]. However, most of them are assuming that the drift value is constant during a relatively long time and hence computing the drift by considering the entire image data even though different part of the image undergoes different drift contamination. In our previous work [25], a local scan method is applied in a nano-robotic manipulation system to manipulate nano-objects with high efficiency and reliable real-time visual feedback during manipulation. By correcting the location of a nano-object in the augmented reality interface during manipulation using the local scan method, the displayed position of the nano-object matches its actual position. Therefore, nanomanipulation performed based on the actual position is much more reliable and has fewer failures. However, the local scan during manipulation may affect the productivity of the manipulation because it takes long time to find the actual location of the object in an AFM image with large drift-contamination, as more scanning lines are needed to search for the nano-object. Therefore, it would be favorable to start the manipulation from a drift contamination free AFM image to minimize the load of local scan during manipulation, as a result, to improve the efficiency of manipulation but maintain the same reliability.

In this paper, a local scan strategy is applied to locally identify and compensate the thermal drift in AFM images such that a drift contamination free AFM image can be obtained before manipulation. The brief process is as follows: First, an AFM image is captured and the entire image is divided into several parts along y direction. Second, a local scan is immediately performed in each part of the image to calculate the value of thermal drift. Finally, by mapping all pixels of each part to a new coordinates corresponding to the calculated thermal drift value, the thermal drift contamination is canceled and a contamination-free image is recovered, leading to improved accuracy for AFM imaging and enhanced productivity for AFM based nanomanipulation.

The rest of this paper is organized as follows: the local scan mechanism is briefly introduced in Section II; the thermal drift problem is presented and the compensation method is proposed in Section III. The system implementation and simulation result are included in Section IV before conclusions in Section V.

II. Local Scan

In our previous research work [25, 26], we have developed a local scan method to realize a real-time visual feedback during manipulation. Instead of scanning an area line by line to recover every details of that location, during manipulation, our local scan method only scans a minimum of two lines for nano-particles and scans a minimum of three lines for nano-rods based on the objects' features. The location of a nano-particle can be approximately represented by its center and radius. The radius of each particle, R, can be identified from the captured AFM image. The actual location of the nano-particle can be recovered with minimum of two scanning lines (Line L_2 and V) as shown in Figure 1.

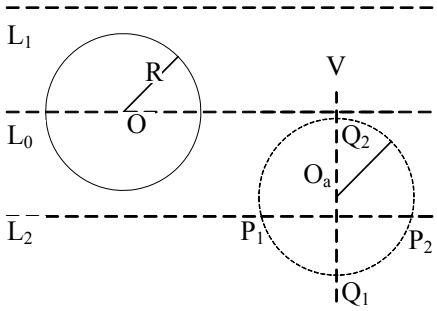

Fig. 1 Local scan of nanoparticles: First, the nano-particle is scanned using Line L_0, which passes through point O, the displayed center of the particle in the original AFM image. If the particle is not found, then the scanning line moves up and down alternatively by a distance of $(3/2)R$ until the particle is found. Once the particle is found, the scanning line forms two intersection points with the boundary of the particle, P_1 and P_2. Additional vertical line, V, which goes through the midpoint between P_1 and $P_2$and perpendicular to the previous scanning line, is scanned to find the actual center of the particle. The vertical scanning line has two intersection points with the boundary of the particle, Q_1 and Q_2. The actual center of the nano-particle, Oa, is located at the midpoint between Q_1 and Q_2. The local scanning range (the length of the scanning line, l) is determined by the maximum random drift such that $l>R+r_{max}$, where r_{max} is the maximum random drift distance.

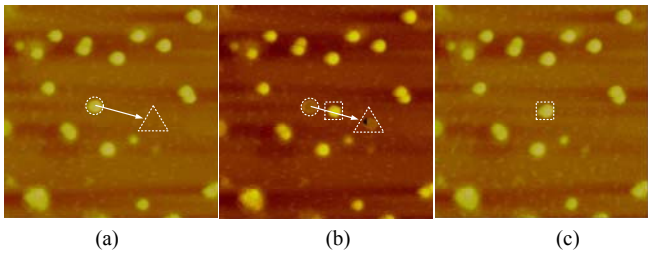

(a) (b) (c)

Figure 2: (a) AFM image of nano-particles before manipulation (the particle inside the circle will be moved; (b) The real-time visual display during manipulation (the particle inside the circle is supposed to be moved into the triangle box, however, it is found inside the square by local-scan-after-operation); (c) The AFM image after manipulation. The scanning range of the image is 3μm£3μm.

The experimental results of local scan in manipulation of nanoparticles with local-scan-after-operation are shown in Figures 2 & 3. As shown in Figure 2, a particle is pushed from one location to another location. A scanning pattern is generated as shown in Figure 3(a). The local scan results are shown in Figure 3(b). From the local scan information, the actual position of the nano-particle can be easily recovered by the particle center defined by the second scan line.

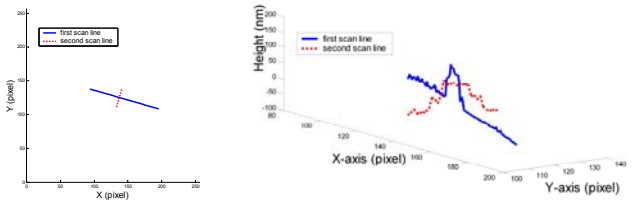

(a) (b)

Figure 3 (a) The local-scan-after-operation pattern for a particle generated according to the local scann strategy. (b) The local-scan-after-operation results of a nano-particle.

When the local scan and manipulation operation are switched back and forth at a video frame rate (larger than 16Hz), the position of the object being manipulated can be updated in real-time. Because the local scan only takes a very small fraction of time at high frequency, it is transparent for operator, i.e. the operator does not notice the local scan is undergoing during operation of manipulation.

In this paper, we will mainly focus on the drift compensation by local scan before manipulation and after object identification which should also be transparent to operators. The purpose of the local scan in this study is to obtain a drift contamination free AFM image by calculating the drift value at each pixel and then compensating it. Starting from a drift contamination free image for nanomanipulation, the operation time of the local scan during manipulation can be significantly reduced, and therefore, the overall manipulation time can also be decreased significantly.

III. Drift Compensation Method

In ambient conditions where the environmental temperature is not tightly controlled, the position of AFM tip relative to stage drifts with time, even though the voltage for controlling the tip position is held constant. The drift velocities on the x-y plane are reported to vary from 0.01~0.1 nm/s [19]. In our experiments, the drift in the x direction is around 0.08nm/s, while the drift in the y direction is around 0.02nm/s. After about ten minutes scan, the drift along x direction can be as much as 50nm, which is comparable with the diameter of the nanoparticles we normally manipulate. Thus, AFM based nanomanipulation operations are fallible and inefficient because objects can be easily missed due to the position errors caused by thermal drift.

There is also drift in the z direction, however, it is very difficult to precisely measure drift in the z direction because the topographic data acquired by an AFM are relative height information of a series of discrete points on the sample

surface. Fortunately, it is usually relatively small (as small as 0.005nm/s [27]) and has little impact on nanomanipulation; moreover, it can be well compensated by the z feedback system. Thus it is normally sufficient to deal with drift in the x and y directions under the existence of drift in z direction, so the nanomanipulation could be performed as if the drift does not exist.

Previous experimental results have shown that the drift along x and y directions is translation and no rotation is involved. Moreover, the correlation between two directions can be negligible [19]. While ignoring the drift long z direction, the height data between two successive scans in a same sample area can be expressed as [27]

$$h_{t+1}(x,y) = h_t(x+\Delta x_t, y+\Delta y_t) \quad (1)$$

Where Δx_t and Δy_t denote drift value in the x and y direction respectively between time instants t and $t+1$. Once Δx_t and Δy_t are calculated, a drift-corrected image can be simply calculated by making coordinates translation for all pixels of the AFM image

$$h_t(x,y) = h_{t+1}(x-\Delta x_t, y-\Delta y_t) \quad (2)$$

Considering the raster scan nature of AFM when acquiring an AFM image, the whole AFM image can be divided into N parts along y direction, as shown in Figure 4. The thermal drift can be considered as the same for each pixel inside the same part, which is reasonable because the image inside that part is captured within a very short time. If a local scan is performed in every part, then the drift in every part can be calculated.

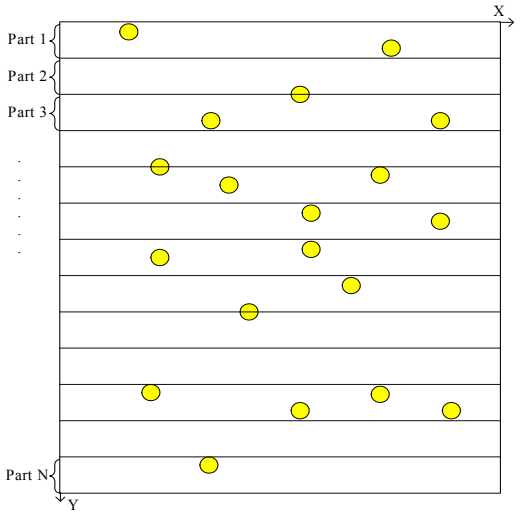

Fig. 4 Scheme of local scan for a whole image: a local scan is performed in every region when there are particles located.

Nano-particles are usually randomly distributed on the substrate before manipulation. It is possible that there is no nano-particle in some parts while there is more than one nano-particle in other parts. For the part without nano-particle, the thermal drift has no effect on the manipulation, thus the drift value can be set equal to that of the nearest neighbour part with nano-particles. For those parts with more than one nano-object, a nano-particle most close to the center of the part will be chosen to perform local scan to calculate the drift values and the drift values for other particles are set same as it. In this manner, the drift values along x and y direction in every part, Δx_{t1}, Δx_{t2} …Δx_{tN} and Δy_{t1}, Δy_{t2}…Δy_{tN}, can be calculated. According to Equation (2), for any part i ($1 \le i \le N$), a coordinate translation for all pixels in this part can be performed using the following equation

$$h_t(x,y) = h_{t+1}(x-\Delta x_{ti}, y-\Delta y_{ti}) \quad (3)$$

The compensating algorithm is explained in details: An AFM image with n×n pixels is represented by a n×n data matrix **A**. Each element in the data matrix represents a corresponding pixel in the image. Let $a_{i,j}$ be the element in ith row and jth column of matrix. The data matrix **A** is divided into N sub-matrixes with dimension of (n/N)×n, each sub-matrix represents an image stripe in Figure 4. Two data matrixes **B** and **C** are introduced, where **B** is the data matrix after x-drift compensation and **C** is the data matrix after y-drift compensation. Similarly, $b_{i,j}$ and $c_{i,j}$ are introduced to represent the element in ith row and jth column of matrix **B** and **C**. The drift values along x and y direction in any sub-matrix s ($1 \le s \le N$) can be calculated as Δx_s and Δy_s by the local scan performed in the corresponding image stripe. Here Δx_s and Δy_s should be integer if we calculate the drift value in pixel. The drift compensation for x direction is performed first. For sub-matrix s, the drift along x direction is Δx_s pixel. Every element in sub-matrix s should be shifted by $-\Delta x_s$ column to compensate the drift. Namely, let

$$(b_{i,j})_s = (a_{i,j+\Delta x_s})_s \quad (4)$$

To make sure that $a_{i,j}$, $b_{i,j}$ are within the range sub-matrix s, restriction $1 \le i \le N$, $1 \le j \le n$ and $1 \le j+\Delta x_s \le n$ should be applied. If $\Delta x_s > 0$, the restriction for j becomes $1 \le j \le n-\Delta x_s$; If $\Delta x_s < 0$, the restriction for j becomes $1-\Delta x_s \le j \le n$. For $\Delta x_s > 0$, $1 \le i \le N$ and $n-\Delta x_s < j \le n$, there is no corresponding elements in the original matrix **A** for $b_{i,j}$, here we define a constant

$$d = \left(\sum_{i,j=1}^{i,j=n} a_{i,j}\right)/(n \times n) \quad (5)$$

and set $b_{i,j}=d$. Similarly, for $\Delta x_s < 0$, $1 \le i \le N$ and $1 \le j < 1-\Delta x_s$ there is no corresponding elements in the original matrix **A** for $b_{i,j}$ and $b_{i,j}$ is set to equal to d.

The drift compensation along y direction is similar to the above procedure. For sub-matrix s, the drift along y direction is Δy_s pixel. Every element in sub-matrix s should be shifted by $-\Delta y_s$ row to compensate the drift. Namely, let

$$(c_{i,j})_s = (b_{i+\Delta y_s,j})_s \quad (6)$$

To make sure that $b_{i,j}$, $c_{i,j}$ are within the range of sub-matrix s, restriction $1 \leqslant i \leqslant N$, $1 \leqslant i + \Delta y_s \leqslant N$ and $1 \leqslant j \leqslant n$ should be applied. If $\Delta y_s > 0$, the restriction for i becomes $1 \leqslant i \leqslant N - \Delta y_s$; If $\Delta y_s < 0$, the restriction for i becomes $1 - \Delta y_s \leqslant i \leqslant N$. For $\Delta y_s > 0$, $N - \Delta y_s < i \leqslant N$ and $1 \leqslant j \leqslant n$, there is no corresponding elements for $c_{i,j}$ in the sub-matrix s of **B**. Considering that the last rows in sub-matrix s are adjacent to the first rows in sub-matrix $s+1$, here we set

$$(c_{N-\Delta y_s+1,\,j})_s = (b_{1,j})_{s+1} \qquad (7)$$

$$(c_{N-\Delta y_s+2,\,j})_s = (b_{2,j})_{s+1} \qquad (8)$$

$$\vdots$$

$$(c_{N,j})_s = (b_{\Delta y_s,\,j})_{s+1} \qquad (9)$$

The above equations are valid if $s<N$. For $s=N$, there is no adjacent rows for last rows in sub-matrix N, here we set every element in row $N-\Delta y_s+1$, $N-\Delta y_s+1,\ldots,N$ equal to constant d.

Similarly, for $\Delta y_s < 0$, $1 \leqslant i < 1 - \Delta y_s$ and $1 \leqslant j \leqslant n$, if $s>1$, we set

$$(c_{1,j})_s = (b_{N-\Delta y_s,\,j})_{s-1} \qquad (10)$$

$$(c_{2,j})_s = (b_{N-\Delta y_s+1,\,j})_{s-1} \qquad (11)$$

$$\vdots$$

$$(c_{\Delta y_s,\,j})_s = (b_{N,j})_{s-1} \qquad (12)$$

if s=1, there is no adjacent rows for first rows in sub-matrix 1, we set every element in row1, 2,…, Δy_s equal to constant d.

After performing the coordinate translation, the drift effect can be compensated and a drift-contamination free image can be obtained. Increasing N may lead to improved estimation of the drift value. However, it is not always true since the AFM undergoes drift as well when performing the local scan. The operation time of local scan is around 2 seconds for N equal to 16 in our study. It is negligible while compared with the time of acquiring an AFM image, which is around 300 seconds in our experiments. Thus, the drift during local scan can be ignored for relatively small N. As the N increase, the time for local scan will increases drastically and is no longer negligible, leading to inaccurate estimation of drift value. There is a trade-off between N and the accuracy, so N should be properly chosen to achieve optimal accuracy.

IV System Implementation and Simulation Result

An AFM based nano-robotic system assisted by augmented reality has been developed in our precious work [5, 12], which is implemented on a Veeco Scanning Probe Microscope (Bioscope AFM). In this paper, the augmented reality enhanced interface is implemented on an Agilent 5500 Scanning Probe Microscope [25]. The infrastructure of the nano-robotic system is still the same as before. As shown in Figure 5, the nano-robotic system includes three subsystems: the AFM system, the real-time control module and the augmented reality interface.

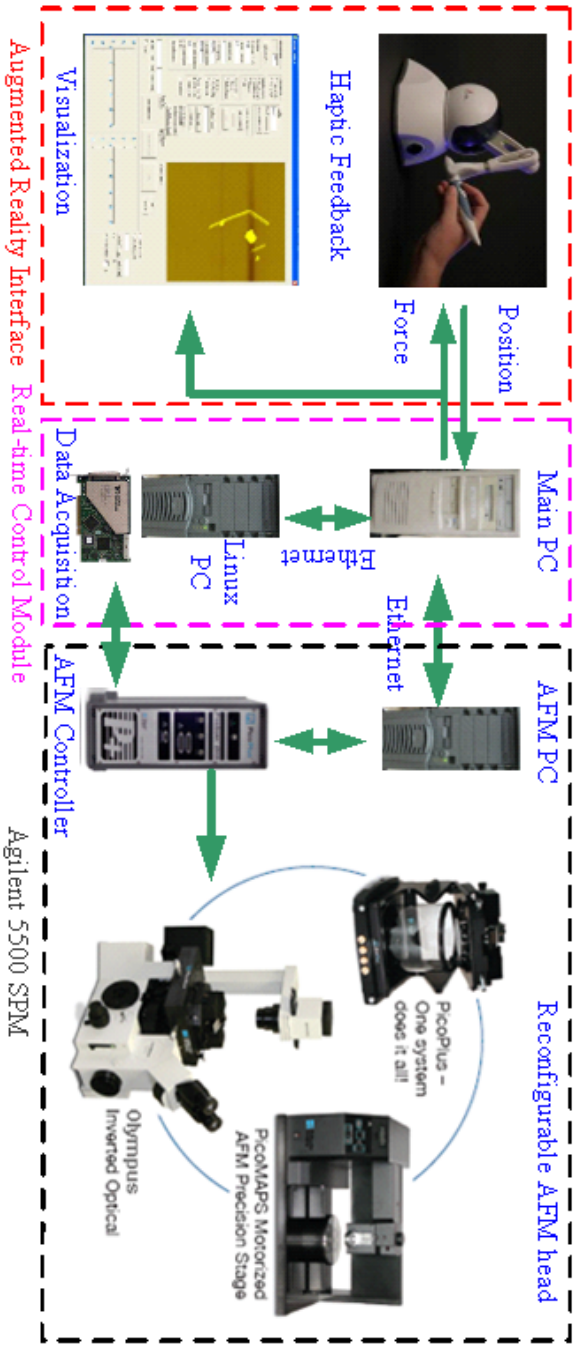

Fig. 5 The AFM based nano-robotic system. Right: the AFM system including other accessories for imaging functions and control modules; Left: the augmented reality interface that provides an environment for an operator to simultaneously control the tip motion through a haptic joystick, view the real-time AFM image, and feel the real-time force during manipulation.

The AFM system includes the AFM head, AFM PC, AFM controller. The AFM head is equipped with a close-loop scanner with a maximum X×Y scan range of 90 μm×90μm and a Z scan range of 7μm. Peripheral devices include an Olympus inverted optical microscope (Olympus IX71). The inverted optical microscope helps the operator to locate the tip, point the laser beam to the cantilever, and search for the interesting areas on substrate. The AFM PC is responsible for running main control program and providing an interface for the imaging. The real-time control module has a data acquisition card (PCI-DAS4020/12, Measurement Computing Co.) inside. It is responsible for running the local scan program to locate the actual position of the nano-object and update it to the Main PC via Ethernet. The augmented reality interface consists of a haptic device (Phantom^{TM} from Sensable Co.) and a nanomanipulation program running on the main PC. The augmented reality interface provides both real-time visual and force feedback for the operator to view real-time AFM image at video frame rate and feel the force feedback during nanomanipulation. The haptic device serves as the force feedback device. It also works as a joystick, through which the operator can input the position command. The real-time visual display is a dynamic AFM image of the operating environment which is locally updated based on the preacquired environment information, tip-object interaction model, nano-objects' behavior models, real-time force information, and local scanning information.

A simulation of drift compensation process is performed to verify the feasibility of the drift elimination method. A drift-contaminated AFM image with 256 × 256 pixels is shown in Figure 6 (a). To compensate the drift, this image is divided into 16 stripes along y direction (Here the coordinate system is the same as in Figure 4). Assuming the drift value in stripe 1, 2, 3…16 is -1, -2, -3…-16 pixels along x direction. The drift value along y direction is relatively small, thus we assume for stripe 1 to 4, there is no drift in y direction, and for stripe 5 to 8, the drift along y direction is -1 pixel, for stripe 9 to 12, the drift along y direction is -2 pixels, and for stripe 13 to 16, the drift along y direction is -3 pixels. The drift compensation process is simulated using the algorithm stated in Section III part B. The simulation result is shown in Figure 6 (b). As long as the drift contamination is eliminated, the nanomanipulation based on the AFM image of nano-particles can be accurate and efficient.

IV Conclusions

In this study, a local scan strategy has been proposed to eliminate the drift contamination in AFM images. By dividing the AFM image into many parts along y direction, the local scan in each part can calculate the drift value at that part. After compensating the drift in each part using our proposed algorithm, a drift contamination free image can be recovered simply from a coordinate transformation equation. The AFM based nanomanipulation will become more reliable and efficient based on a drift contamination free image. A simulation process has demonstrated the feasibility of the drift elimination method. In our future study, we will perform the experiment to verify the effectiveness of our proposed local scan strategy in elimination of drift contamination in AFM images for nanomanipulation.

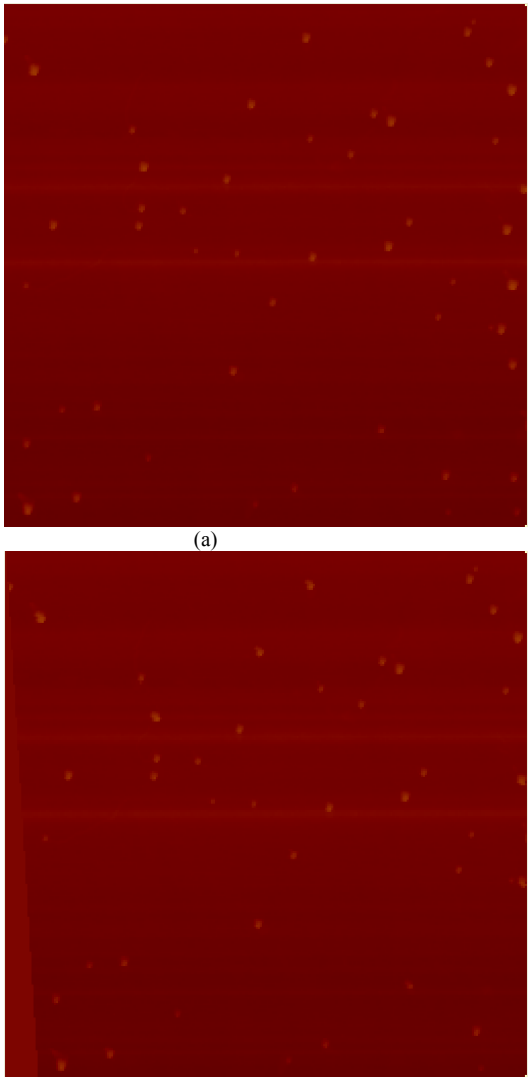

(a)

(b)

Fig. 6 (a) An AFM image of latex nano-particles before drift compensation. (b) The image after drift compensation. The image area is 5um × 5um, the diameter of the latex particle is around 50nm.

References

[1] G. Binning, C. F. Quate, and C. Gerber, "Atomic force microscope,"Phys. Rev. Lett., vol. 56, no. 9, pp. 930–933, 1986.

[2] D. Wang, L. Tsau, K. L. Wang, and P. Chow, "Nanofabrication of thin chromium film deposited on si(100) surfaces by tip induced anodization in atomic force microscopy," Appl. Phys. Lett., vol. 67, pp. 1295–1297, 1995.

[3] D. M. Schaefer, R. Reifenberger, A. Patil, and R. P. Andres, "Fabrication of two-dimensional arrays of nanometer-size clusters with the atomic force microscope," Appl. Phys. Lett., vol. 66, pp. 1012–1014, Feb. 1995.

[4] T. Junno, K. Deppert, L. Montelius, and L. Samuelson, "Controlled manipulation of nanoparticles with an atomic force microscope," Appl. Phys. Lett., vol. 66, no. 26, pp. 3627–3629, Jun. 1995.

[5] G. Y. Li, N. Xi, H. P. Chen, et al, ""Videolized" Atomic Force Microscopy for interactive nanomanipulation and nanoassembly", IEEE Trans. on Nanotechnology, Vol. 4, No. 5, Sep. 2005
[6] T. Junno, K. Deppert, L. Montelius, and L. Samuelson, "Controlled manipulation of nanoparticles with an atomic force microscope," Appl. Phys. Lett., vol. 66, no. 26, pp. 3627–3629, Jun. 1995.
[7] D. M. Schaefer, R. Reifenberger, A. Patil, and R. P. Andres, "Fabrication of two-dimensional arrays of nanometer-size clusters with the atomic force microscope," Appl. Phys. Lett., vol. 66, pp. 1012–1014, Feb. 1995.
[8] R. W. Stark, S. Thalhammer, J.Wienberg, and W. M. Heckl, "The AFM as a tool for chromosomal dissection-the influence of physical parameter," Appl. Phys. A, vol. 66, pp. 579–584, 1998.
[9] M. Sitti and H. Hashimoto, "Tele-nanorobotics using atomic force microscope," in Proc. IEEE Int. Conf. Intelligent Robots and Systems, 1998, pp. 1739–1746.
[10] M. Falvo, R. Superfine, S.Washburn, M. Finch, R. Taylor, V. Chi, and F. B. Jr, "The nanomanipulator: A teleoperator for manipulating materials at the nanometer scale," in Proc. Int. Symp. Science and Technology of Atomically Engineered Materials, 1995, pp. 579–586.
[11] M. Sitti and H. Hashimoto, "Controlled pushing of nanoparticles: Modeling and experiments," IEEE/ASME Trans. Mechatron., vol. 5, pp. 199–211, Jun. 2000.
[12] G. Y. Li, N. Xi, and M. Yu, "Development of augmented reality system for AFM based nanomanipulation," IEEE/ASME Trans. Mechatron., vol. 9, pp. 358–365, Jun. 2004.
[13] G. Y. Li, N. Xi, M. Yu, and W. K. Fung, "Augmented reality system for real-time nanomanipulation," presented at the IEEE Int. Conf. Nanotechnology, San Francisco, CA, 2003.
[14] B. Mokaberi and A. A. G. Requicha, "Towards automatic nanomanipulation: Drift compensation in scanning probe microscopes," in Proc. IEEE Int. Conf. Robotics and Automation, 2004, pp. 416–421.
[15] W. Vogl, B. Ma, and M. Sitti, "Augmented Reality User Interface for an Atomic Force Microscope based Nanorobotic System," IEEE Trans. on Nanotechnology, vol. 5, no. 4, pp. 397-406, 2006.
[16] M. Sitti and H. Hashimoto, "Teleoperated Touch Feedback of Surfaces at the Nanoscale: Modeling and Experiments," IEEE/ASME Trans. on Mechatronics, vol. 8, no. 2, 2003.
[17] A. A. G. Requicha, "Nanorobots, NEMS and Nanoassembly," Proc. IEEE, vol. 91, No. 11, pp. 1922-1933, 2003
[18] L. Liu, N. Xi, Y. Luo, J. Zhang, G. Li. Sensor Referenced Guidance and Control for Robotic Nanomanipulation. IEEE/RSJ 2007 International Conference on Intelligent Robots and Systems. Oct. 29~Nov. 2, 2007, San Diego, CA
[19] B. Mokaberi and A. A. G. Requicha, "Drift compensation for automatic nanomanipulation with scanning probe microscopes", IEEE Trans. on Automation Science & Engineering, Vol. 3, No. 3, pp. 199-207, July 2006
[20] V. Y. Yurov and A. N. Klimov, "Scanning tunneling microscope calibration and reconstruction of real image: Drift and slope elimination," Rev. Sci. Inst., vol. 65, No. 5, pp. 1551-1557, 1994.
[21] R. Staub, D. Alliata and C. Nicolini, "Drift elimination in the calibration of scanning probe microscopes," Rev. Sci. Inst. vol. 66, no. 3, pp. 2513-2516, 1995.
[22] J. T. Woodward and D. K. Schwartz, "Removing drift from scanning probe microscope images of periodic samples," J. Vac. Sci. Technol. B, vol. 16, no. 1, pp.51-53, 1998.
[23] S. H. Huerth and H. D. Hallen, "Quantitative method of image analysis when drift is present in a scanning probe microscope," J. Vac. Sci Technol. B, vol. 21, no. 2, pp. 714-718, 2003.
[24] K. J. Ito, Y. Uehara, S. Ushioda and K. Ito, "Servomechanism for locking scanning tunneling microscope tip over surface nanostructures," Rev. of Sci. Inst., vol. 71, no. 2, pp. 420-423, 2000.
[25] G. Li, L. Liu, and N. Xi, "Augmented Reality Enhanced Nanomanipulation by Atomic Force Microscopy with Local Scan", the 2007 International Manufacturing Science & Engineering Conference (IMSEC). October 15-18, 2007 in Atlanta, GA.
[26] L. Liu; Y. Luo; N. Xi; Y. Wang; J. Zhang; G. Li. "Sensor Referenced Real-Time Videolization of Atomic Force Microscopy for Nanomanipulations." IEEE/ASME Trans. Mechatron vol 13, pp. 76-85, Feb 2008
[27] Q. Yang, S. Jagannathan and E.W. Bohannan, "Block Phase Correlation-based Automatic Drift Compensation for Atomic Force Microscopes", Proceedings of 2005 5th IEEE Conference on Nanotechnology, Nagoya, Japan, July 2005